

Synthesis of Silver Nanoparticles from *Mimusops elengi* Extract of Raw Fruits and Characterization of PVA-Silver Polymer Nanocomposite Films

BHABANI SHANKAR PANDA^{1,*} and MOHAMMED ANSAR AHEMAD²

¹Coastal Laboratory, State Pollution Control Board, Integrated Coastal Zone Management Project (ICZMP), Bhubaneswar-751024, India

²Department of Chemistry, Gandhi Institute for Education and Technology, Bhubaneswar-752060, India

*Corresponding author: E-mail: bpanda607@gmail.com

Received: 18 November 2020;

Accepted: 14 January 2021;

Published online: 20 March 2021;

AJC-20279

The present work concerns on the synthesis of silver nanoparticles at 25 °C using raw fruits extract of Bakul (*Mimusops elengi*) tree via chemical reduction route development of poly(vinyl alcohol) PVA-silver polymer nanocomposite films. The nanocomposite films were subjected to characterization by UV-visible, FTIR, X-ray diffraction, field emission scanning electron microscope (FESEM) and thermal studies. The UV-visible spectrum shows a characteristic broad absorption band observed near 465 nm suggesting presence of silver nanoparticles in polymer nanocomposites (PNCs) film. The vibrational band shift of –OH group of poly(vinyl alcohol) in the presence of nanoparticle designated the chemical interaction between –OH group of poly(vinyl alcohol) and silver nanoparticles. The FESEM study confirmed that PVA is not only acted as a capping agent, but also a cross-linking agent. X-ray diffraction study shows that the existence of AgNPs in the poly nanocomposite film and nanoparticles are crystalline in nature. Thermal studies suggest that the enhanced thermal stability is because of the good packing of the polar crystallites in β -PVA composites as compared to the non-polar α -phase of neat poly(vinyl alcohol) (PVA).

Keywords: Raw fruits extract, *Mimusops elengi*, Polymer nanocomposites, Nanofluids, Silver nanoparticles.

INTRODUCTION

Nanotechnology has gained remarkable attention over time. It is a multiphase solid material in which dispersion phase material, which dispersed in a matrix material is in nanoscale [1-3]. So, it forms by dispersing a nanomaterial into other distinct materials. The importance of this material is that two components have a very small interaction between the individual components having unique structures over an extended scale at a nonmetric level. The phases might be a solid, a liquid or combination of both. Moreover, the nanocomposites used to exploit towards producing homogeneously large-grained constituents resulting conservative bulk composite or materials with useful new properties. In recent years, metal nanoparticles are widely used in various potential fields such as sensing, optoelectronics, catalysis, lubrication, electromagnetic interference shielding, solar cells, water treatment, *etc.* due to possession of interesting physical and chemical properties quite different from those in the bulk material [4-11].

The addition of nanofillers show incredible upgrading in the properties of the polymer. The use of nanofillers lowers the content loading on the polymer matrix than that of the use of microfillers [12]. For the study of their uses in different fields various researches have been carried out for the synthesis of a large number of polymeric nanocomposites. Different types of polymers (such as polyaniline, polyvinyl alcohol (PVA), polyethylene (PE), polyvinylidene fluoride (PVDF), polyvinyl chloride (PVC), polyamide, *etc.*) are encumbered with several types of nano fillers like Cu₂O, FeO, ZnS, CdS, graphene oxide, *etc.* for the development in structural, optical, mechanical and electrical properties of polymer nanocomposites (PNCs) [12, 13]. Wang *et al.* [14] reported that using a simple and practical approach, one can synthesize polymer composites where PVA is the matrix and graphene acts as reinforcing agent. PVA/Cu₂O PNCs films were set up by light of γ -ray [15]. They found that such PNCs film can be utilized for the radiation location and individual dosimeter in country areas and low monetary nations. Saini *et al.* [16] used PVA grafted silicon carbide nanocrystals

for the improvement of the properties of PVA. By a hydrothermal process, PVA based iron sulfide, cobalt and nickel nanocomposites were also prepared as reported by Qian *et al.* [17]. Krkljes *et al.* [18] reported the Ag-PVA polymeric nanocomposites loaded with various Ag-contents and γ -radiations was utilized to decrease silver particles in the presence of PVA arrangement in water.

In this work, silver nanoparticles (AgNPs) were obtained from the raw fruit extract of Bakul tree (*Mimusops elengi*). The extract was acted as a stabilizing agent as well as reducing agent in aqueous medium. The prepared silver nanoparticles were further utilized in the preparation of Ag-PVA polymeric nanocomposite films.

EXPERIMENTAL

Fruit extract: The raw fruits of *Mimusops elengi* (10 g) were collected from the local orchid area, washed thoroughly and placed in a beaker in 100 mL deionized water. The beaker covered with watch glass was then placed in a hot plate containing magnetic stirrer at 80-85 °C for 1 h and 20 min. The aqueous extract was filtered using Whatman filter paper No. 42 (2.5 μ m) and kept in a refrigerator 10-12 °C.

Synthesis of AgNPs: Aqueous extract (5 mL) in a beaker was placed on the hotplate at 75 °C with magnetic stirrer followed by the addition of silver nitrate solution dropwise. Five samples were prepared by adding 0.05, 0.1, 0.15, 0.2 and 0.25 mL of silver solution. The colour of the solution was changed to brown due to formation of silver nanoparticles.

Development of Ag-PVA PNC films: Nanofluids consisting of different amount *i.e.* 0.5, 1.0, 1.5, 2.0 and 2.5 mL were added to a fixed volume of PVA solution. For the development of PNCs, the nanofluids in petri dishes were kept at 90 °C for 10 h for complete evaporation of the solvents and finally kept for characterization.

The optical absorption analysis was conducted in an ultra violet spectrometer or UV-Visible spectrometer (Perkin-Elmer Lambda 750 spectrophotometer) in the range of 200-900 nm.

The FTIR analysis was conducted in the range of 4000-400 cm^{-1} using Perkin-Elmer Model: Spectrum-65. The crystalline structures of silver nanoparticles were studied as a wide angle with the help of an X-ray diffractometer (Make: Philips; model: PW-1710). The diffracted data were noted using a filtered monochromatic radiation of $\text{CuK}\alpha$ having the wavelength (λ) range 0.15405 nm over a Ni filter. The data were collected with a computer, which was bordered over the diffractometer, at a scanning speeds of 0.05°/s in applied current 20 mA and applied voltage of 40 kV. The range of the diffraction angle, which is denoted as 2θ wide-ranging from 10° to 100°. In a crystalline phase, the average crystallite size (D) can be studied from the peak-thicknesses in the characteristic XRD peaks using the formula derived by Debye-Scherrer [19]. The field emission scanning electron microscopic (FESEM) images of discriminatory samples of polyananocomposite films were taken at discriminatory scales of magnifications of some of samples [20] (make: The Oxford model Leo1550 VP-SEM). The images were taken at an augmented voltage range of 2 to 10 kV. The thermal analysis were conducted by heating 10 to 30 mg of sample (powder or pieces of films) in an aluminum pan over 300 to 900 K under a pure argon atmosphere (make: Perkin-Elmer, Model: DT-40, Shimadzu Co. Japan).

RESULTS AND DISCUSSION

UV-visible studies: At room temperature, the UV-visible optical absorption spectra in the range of 200 to 900 nm were studied to authenticate the development of AgNPs in the PVA-Ag PNC films. The absorption spectra of five poly nanocomposite film samples consisting of (a) 0 mm, (b) 10 mm, (c) 20 mm, (d) 30 mm and (e) 50 mm AgNPs, respectively are shown in Fig. 1a. Two types of absorption bands were detected in the UV spectrum. One type of band is weak band; which is found at 199 nm from $n \rightarrow \pi^*$ electronic transition of the PVA polymer [21,22]. Another broad found near 465 nm is attributed to SPR band. For PVA without AgNPs, no SPR band is detected. From Fig. 1b, it is observed that with increasing the

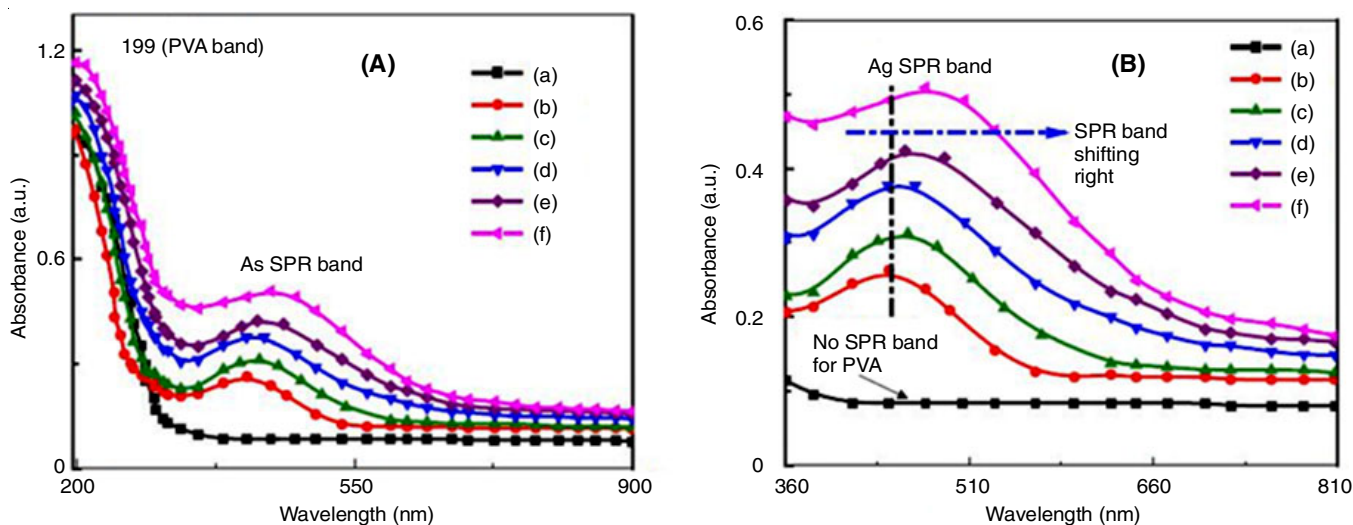


Fig. 1. (A) UV-visible absorption spectra of PVA-Ag PNCs containing (a) 0 mm, (b) 10 mm, (c) 20 mm, (d) 30 mm and (e) 50 mm Ag NPs; (B) SPR band of PNCs consisting of (a) 0 mm, (b) 10 mm, (c) 20 mm, (d) 30 mm and (e) 50 m Ag NPs

contents of AgNPs, the intensity of SPR band increased [23-26]. It is obvious that with the increase in the silver content, definitely there will be a decrease in the absolute number of PVA molecules, which form particle size to increase. Also, near 199 nm, the intensity of band increased with increasing the content of nanoparticles. It clearly recommends that nanoparticles helps the PVA molecules to absorb UV-light strongly in the lower wavelength region.

FTIR analysis: The interfacial interaction between AgNPs and PVA was studied using FTIR spectroscopy. The FTIR spectra of five films consisting of different amount of AgNPs in PVA nanocomposite films are shown in Fig. 2. The various FTIR bands of neat PVA polymer shows bands at 3450, 3080, 2895, 1535, 1470, 1510, 1360, 1195 and 684 cm^{-1} . A relatively broad and intense band appeared between 3500-3200 cm^{-1} due to O-H stretching vibration indicates the presence of polymeric association of the free hydroxyl groups and bonded O-H stretching vibration. Whereas the bands at 1550-630 cm^{-1} suggests that O-H plane bending motion is coupled strongly with other molecular motions [27]. The symmetric CH_2 stretching bands of CH_2 group a different absorption band occurred at 2877 cm^{-1} [28-30]. Also, the intensity of some selective vibrational band (C-H_2 bending) has increased drastically at 1475 cm^{-1} in presence of AgNPs. The carbonyl group is appeared at 1692 cm^{-1} and at 1146 cm^{-1} , the C-O stretching vibration of the ether group takes place [31,32]. These bands originate in the spectra tells that PVA is present in the polymer nanocomposite films.

FESEM analysis: The morphology, size distribution and size of the AgNPs were examined using FESEM images. The FESEM images (5 μm and 500 nm) of PVA-Ag PNCs films no AgNPs (3a-b); 20 mm AgNPs (3c & d) and 50 mm AgNPs (3e & f) containing 3.0 g/L PVA are shown. In Fig. 3a-b, no particle linkage is found, since films contained only PVA and THF solution. In Fig. 3c-d, the particles were interconnected

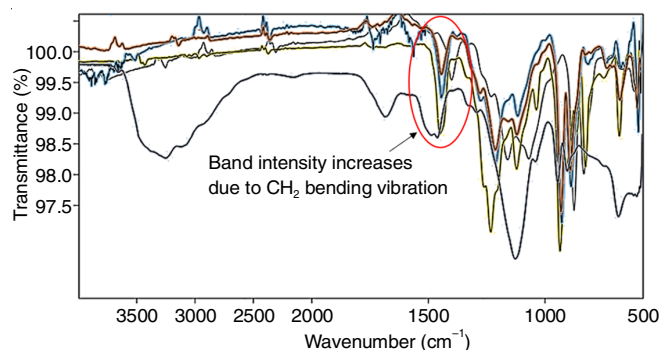


Fig. 2. FTIR spectra of five PVA-Ag PNCs films consisted of (a) 0 mm, (b) 10 mm, (c) 20 mm, (d) 30 mm and (e) 50 mm AgNPs

i.e. AgNPs were crosslinked by PVA polymer. The particles are needle shaped and their average diameter lies in 400-600 nm, however the sizes are not uniformly distributed. In Fig. 3e-f, certain pores and nanoparticles were of non-spherical in shape and some needle like shapes are found.

XRD studies: The diffraction patterns were verified using a filtered monochromatic radiation of $\text{CuK}\alpha$ of $\lambda = 0.15405$ nm through a Ni filter by casting the samples on the Si plate at a scanning angle (2θ) of 100° to 1000° scanning speed of 0.05 m/s and voltage of 40 kV to current 20 mA. The average particle size (D) of AgNPs has been determined by using the Scherrer formula, $D = 0.89\lambda/\beta\cos\theta$. The XRD pattern of neat PVA displays that PVA is crystalline in nature in THF and has only α -phase. At 21.9° , the peak from (110) plane recommend the development of α -phase and no other peak from NPs was observed [33]. A sample containing AgNPs, the peak at 24.3° is from (208) plane of β -phase. The peaks which were observed at 36.21° , 42.73° , 64 and 50.54° matched well with a cubic phase of Ag (Fig. 4). These peaks correspond to the (117), (118) and (138) peaks of crystallite fcc AgNPs present in the PVA matrix [34-36]. From the XRD pattern of AgNPs

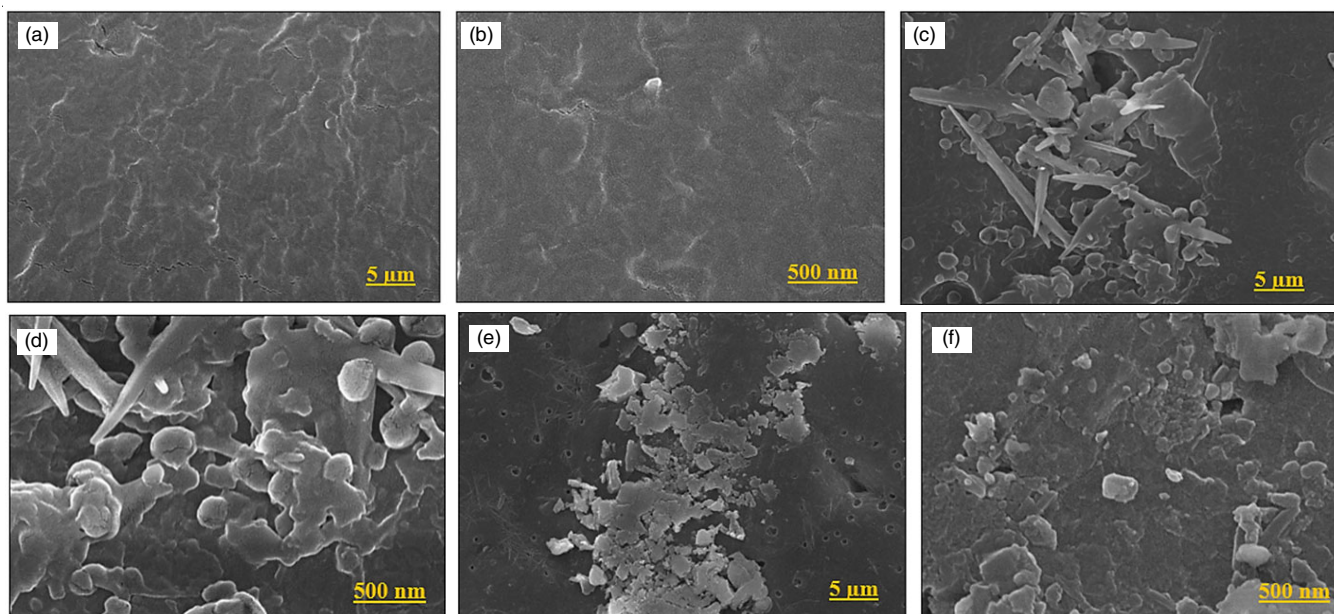


Fig. 3. FESEM image (5 μm and 500 nm) of PVA-Ag PNCs films containing (a & b) 0.0 mm (c & d) 20 mm and (e & f) 50 mm AgNPs

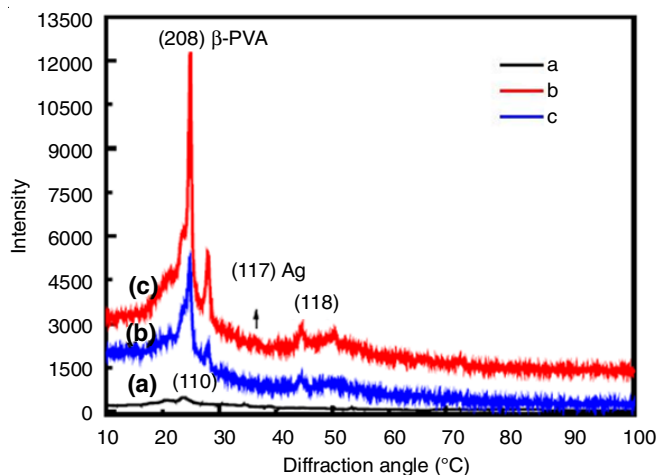


Fig. 4. XRD patterns of selective samples containing 0.0 mm, 20 mm and 50 mm AgNPs

without PVA, no change in the X-ray diffraction pattern was observed. This recommends that the crystalline nature of AgNPs are not concerned by PVA.

Thermogravimetric analysis: Fig. 5 shows the dissimilarity of weight loss (%) in contrast to temperature for neat PVA and PNC films. From the thermograms, it is observed that samples were thermally stable in the temperature ranges 55–450 °C. PVA starts degrading (T_{onset}) at 435 °C and continued up to 650 °C. For PNC films, the degradation temperature starts 484 °C for a PNC film containing 50 mm AgNPs. This is due to formation of cross-linked structure between AgNPs and PVA polymer and thus thereby exhibit high strength. The FTIR and XRD studies also suggested that the formation of highly polar β -PVA phase in the PNC film helps in the enhancement of packing of nanoparticles in PVA medium and thereby increasing the thermal stability [37].

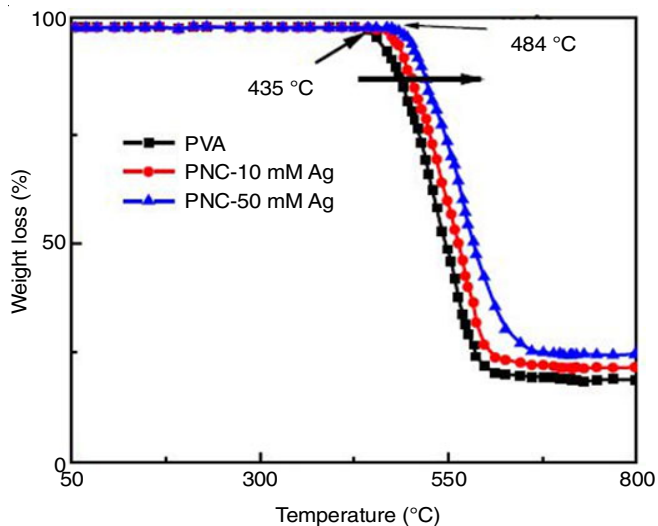


Fig. 5. TGA curve of neat PVA and PVA with AgNPs: (a) PVA, (b) PVA with 10 mm AgNPs and (c) PNC with 50 mm AgNPs

Conclusion

The synthesized silver nanoparticles from the *Mimusops elengi* extract of raw fruits as capping agent and hydrazine

as a reducing agent were incorporated in order to develop the poly(vinyl alcohol)-silver nanoparticles nanocomposite (PNC) films. The UV-visible and X-ray diffraction analyses confirmed the formation of AgNPs in the film. The FTIR revealed the interaction occurred between silver nanoparticles and PVA polymer. Thermal study suggested that the presence of nanoparticles helps in increasing the thermal stability of PNC films.

ACKNOWLEDGEMENTS

The authors are grateful to Dr. M. Behera, Department of Basic Sciences & Humanities, Silicon Institute of Technology, Bhubaneswar and Dr. S.K. Biswal, School of Applied Sciences, Centurion University of Technology and Management, Bhubaneswar, India who help us to accomplish this research work.

CONFLICT OF INTEREST

The authors declare that there is no conflict of interests regarding the publication of this article.

REFERENCES

- I. Khan, K. Saeed and I. Khan, *Arab. J. Chem.*, **12**, 908 (2019); <https://doi.org/10.1016/j.arabjc.2017.05.011>
- J. Jeevanandam, A. Barhoum, Y.S. Chan, A. Dufresne and M.K Danquah, *Beilstein J. Nanotechnol.*, **9**, 1050 (2018); <https://doi.org/10.3762/bjnano.9.98>
- Q. Wu, W.-S. Miao, Y.-D. Zhang, H.-J. Gao and D. Hui, *Nanotechnol. Rev.*, **9**, 259 (2020); <https://doi.org/10.1515/ntrev-2020-0021>
- P.H.C. Camargo, K.G. Satyanarayana and F. Wypych, *Mater. Res.*, **12**, 1 (2009); <https://doi.org/10.1590/S1516-14392009000100002>
- W. Choi, I. Lahiri, R. Seelaboyina and Y.S. Kang, *Crit. Rev. Solid State Mater. Sci.*, **35**, 52 (2010); <https://doi.org/10.1080/10408430903505036>
- A.T. Odularu, *Bioinorg. Chem. Appl.*, **2018**, 9354708 (2018); <https://doi.org/10.1155/2018/9354708>
- O. Zaytseva and G. Neumann, *Chem. Biol. Technol. Agric.*, **3**, 17 (2016); <https://doi.org/10.1186/s40538-016-0070-8>
- G. Vinci and M. Rapa, *Bioengineering*, **6**, 10 (2019); <https://doi.org/10.3390/bioengineering6010010>
- F. Hussain, M. Hojjati, M. Okamoto and R.E. Gorga, *J. Compos. Mater.*, **40**, 1511 (2006); <https://doi.org/10.1177/0021998306067321>
- R. Das, M.E. Ali, S.B.A. Hamid, S. Ramakrishna and Z.Z. Chowdhury, *Desalination*, **336**, 97 (2014); <https://doi.org/10.1016/j.desal.2013.12.026>
- A.A. Yetisgin, S. Cetinel, M. Zuvun, A. Kosar and O. Kutlu, *Molecules*, **25**, 2193 (2020); <https://doi.org/10.3390/molecules25092193>
- D.R. Paul and L.M. Robeson, *Polymer*, **49**, 3187 (2008); <https://doi.org/10.1016/j.polymer.2008.04.017>
- J.H. Koo, *Polymer Nanocomposites*, McGrawHill Professional Publ., (2006).
- J. Wang, X. Wang, C. Xu, M. Zhang and X. Shang, *Polym. Int.*, **60**, 816 (2011); <https://doi.org/10.1002/pi.3025>
- M.A. Omer and E.A. Bashir, *J. Radiation Res. Appl. Sci.*, **11**, 237 (2018); <https://doi.org/10.1016/j.jrras.2018.03.001>
- I. Saini, A. Sharma, R. Dhiman, S. Aggarwal, S. Ram and P.K. Sharma, *J. Alloys Compd.*, **714**, 172 (2017); <https://doi.org/10.1016/j.jallcom.2017.04.183>
- X.F. Qian, J. Yin, Y.F. Yang, Q.H. Lu, Z.K. Zhu and J. Lu, *J. Appl. Polym. Sci.*, **82**, 2744 (2001); <https://doi.org/10.1002/app.2127>

18. A.N. Krklješ, M.T. Marinovic-Cincovic, Z.M. Kacarevic-Popovic and J.M. Nedeljkovic, *Eur. Polym. J.*, **43**, 2171 (2007); <https://doi.org/10.1016/j.eurpolymj.2007.03.023>
19. S.K. Chatterjee, X-Ray Diffraction: Its Theory and Applications, PHI Learning Pvt. Ltd. (2010).
20. O.C. Wells, Scanning Electron Microscopy, McGraw Hill: New York (1974).
21. A.A. Salisu, H. Abba and M.S. Inuwa, *Int. J. Eng. Appl. Sci.*, **2**, 109, (2015).
22. B.S. Panda, M.A. Ahemad and L.N. Mishra, *Int. J. ChemTech Res.*, **14**, 16 (2021).
23. K. Jyoti, M. Baunthiyal and A. Singh, *J. Radiat. Res. Appl. Sci.*, **9**, 217 (2016); <https://doi.org/10.1016/j.jrras.2015.10.002>
24. Z. Zaheer and Rafiuddin, *Colloids Surf. B Biointerfaces*, **90**, 48 (2012); <https://doi.org/10.1016/j.colsurfb.2011.09.037>
25. S. Moharana and R.N. Mahaling, *Chem. Phys. Lett.*, **680**, 31 (2017); <https://doi.org/10.1016/j.cplett.2017.05.018>
26. J. Audoit, L. Laffont, A. Lonjon, E. Dantras and C. Lacabanne, *Polymer*, **78**, 104 (2015); <https://doi.org/10.1016/j.polymer.2015.09.062>
27. A.M. Shehap, *Egypt. J. Solids.*, **31**, 75 (2008).
28. M. Maity, S.K. Pramanik, U. Pal, B. Banerji and N.C. Maiti, *J. Nanopart. Res.*, **16**, 2179 (2014); <https://doi.org/10.1007/s11051-013-2179-z>
29. M.L. Bhaisare, M.S. Khan, S. Pandey, G. Gedda and H.F. Wu, *RSC Adv.*, **7**, 23607 (2017); <https://doi.org/10.1039/C6RA28705K>
30. C.S. Liyanage, S.N. De Silva and C.A. Fernando, *Int. J. Nanoelectron. Mater.*, **11**, 129 (2018).
31. P. Li, W. Lv and S. Ai, *J. Exp. Nanosci.*, **11**, 18 (2016); <https://doi.org/10.1080/17458080.2015.1015462>
32. A. Muthuvinothini and S. Stella, *Asian J. Chem.*, **31**, 109 (2019); <https://doi.org/10.14233/ajchem.2019.21578>
33. F.S. Al-Hazmi, D.M. de Leeuw, A.A. Al-Ghamdi and F.S. Shokr, *Curr. Appl. Phys.*, **17**, 1181 (2017); <https://doi.org/10.1016/j.cap.2017.05.011>
34. M. Behera, S.K. Biswal, B.S. Panda and M.A. Ahemad, *Asian J. Chem.*, **32**, 106 (2019); <https://doi.org/10.14233/ajchem.2020.22344>
35. R. Majumdar, B.G. Bag and P. Ghosh, *Appl. Nanosci.*, **6**, 521 (2016); <https://doi.org/10.1007/s13204-015-0454-2>
36. S. Abdalla, A. Obaid and F.M. Al-Marzouki, *Results Phys.*, **6**, 617 (2016); <https://doi.org/10.1016/j.rinp.2016.09.003>
37. M. Behera, S.K. Biswal, M.A. Ahemad and B.S. Panda, *Biointerf. Res. Appl. Chem.*, **11**, 12584 (2021); <https://doi.org/10.33263/BRIAC115.1258412595>